Macromolecular Bioscience
www.mbs-journal.de

Covalently Cross-Linked Pig Gastric Mucin Hydrogels Prepared by Radical-Based Chain-Growth and Thiol-ene Mechanisms

Jessica S. Brand, Leonard Forster, Thomas Böck, Philipp Stahlhut, Jörg Teßmar, Jürgen Groll, and Krystyna Albrecht**

Mucin, a high molecular mass hydrophilic glycoprotein, is the main component of mucus that coats every wet epithelium in animals. It is thus intrinsically biocompatible, and with its protein backbone and the *o*-glycosidic bound oligosaccharides, it contains a plethora of functional groups which can be used for further chemical modifications. Here, chain-growth and step-growth (thiol-ene) free-radical cross-linked hydrogels prepared from commercially available pig gastric mucin (PGM) are introduced and compared as cost-efficient and easily accessible alternative to the more broadly applied bovine submaxillary gland mucin. For this, PGM is functionalized with photoreactive acrylate groups or allyl ether moieties, respectively. Whereas homopolymerization of acrylate-functionalized polymers is performed, for thiol-ene cross-linking, the allyl-ether-functionalized PGM is cross-linked with thiol-functionalized hyaluronic acid. Morphology, mechanical properties, and cell compatibility of both kinds of PGM hydrogels are characterized and compared. Furthermore, the biocompatibility of these hydrogels can be evaluated in cell culture experiments.

1. Introduction

Hydrogels, strongly hydrogenated 3D networks, are often investigated in the field of tissue engineering. This is due to the availability of numerous cytocompatible cross-linking schemes and their ability to resemble some features of the natural extracellular matrix (ECM).[1] The transport properties of hydrogels are mainly mediated by diffusion, which can be strongly influenced by the material, cross-linking density, and swelling behavior. Essential in hydrogel formation is that the gelation process is cell compatible and potentially toxic steps are minimized.

Free radical polymerization reaction mechanism is frequently used for the synthesis of hydrogels in the biomedical application's field. Whereas the free radical polymerization of vinyl groups such as acrylates forms a network in a random chain-growth mechanism.[2] The thiol-ene cross-linking of multifunctionalized hydrogel–prepolymers occurs via more controllable free radical step-growth mechanism through dimerization between radicals of electron-poor vinyl groups such as allyl or norbornyl residues and thiols.[3] Compared to the radical chain-growth polymerization, the thiol-ene chemistry leads to a more consistent network as nearly complete consumption of reacting species can be achieved, resulting in formation of thioether bridges between two defined functional groups.[4] Both reaction types proved to be suitable for biocompatible hydrogel synthesis and are therefore already widely used in the field of tissue engineering.[5–7]

A variety of natural and synthetic prepolymers with reactive side groups can be used as building blocks for hydrogels. Though synthetic polymers have benefits, such as the possibility of tailored synthesis,[8,9] polymers of natural origin often exhibit inherent cytocompatibility, are readily available, and may exhibit biochemical similarity to the natural extracellular matrix. One example for such a biopolymer that has recently gained interest in the field of medical application is mucin, the main and gel-forming component of mucus. Mucus, an aqueous slippery secretion, serves in living animal as protection of epithelial cells wherever a body part needs to be protected from external influences, for example, shear stress. Among the most important properties attributed to mucins are barrier properties, dynamics, hydration, lubrication, and bioactivity.[10] An additional motivation for the use of mucins in a biomaterial's application is the fact that it is part of the waste after slaughtering, for example, in pig stomachs. In Germany alone, about 55 million pigs were slaughtered in 2019.[11] With an estimated worldwide pig popula-

J. S. Brand, L. Forster, T. Böck, P. Stahlhut, J. Teßmar, J. Groll, K. Albrecht
Department for Functional Materials in Medicine and Dentistry at the Institute of Functional Materials and Biofabrication
and Bavarian Polymer Institute
University of Würzburg
Pleicherwall 2, Würzburg D-97070, Germany
E-mail: juergen.groll@fmz.uni-wuerzburg.de; krystyna.albrecht@fmz.uni-wuerzburg.de

The ORCID identification number(s) for the author(s) of this article can be found under https://doi.org/10.1002/mabi.202100274

DOI: 10.1002/mabi.202100274

tion of ≈650 million animals, mucus is not only readily available, but maximizing the use that is possible to make out of the waste material is also ethically favorable.

Mucin is a large (molecular weight in tens of megadaltons) glycoprotein, with the chemical composition differing depending on location and function in the body. However, a general feature of mucin is a long protein backbone that contains both hydrophobic and charged domains. On the backbone, glycans are bound via *o*-glycosidic bonds which are terminated by a variety of acidic sugars. These oligosaccharides, attached to the protein backbone, build 50–80% of the molecular weight of mucins[12] and can form inter- and intramolecular hydrogen bonds. This ensures high hydration, hydrophilicity, as well as carboxyl and sulfate groups, which give the mucin a negative total charge at neutral pH.[10,13] The application of mucins is therefore diverse, ranging from the use as filters for negatively charged particles,[14] cell or protein repellent coatings,[15,16] treatment of wound infections,[17,18] to biopharmaceutical applications like in creams, masks, and serums with antiaging effect.[19,20] Due to the high possibility of hydration, the literature often mentions "mucin/mucus hydrogels" or reconstituted mucin hydrogels, meaning mucins that have assembled via physical interactions forming a biopolymer-based hydrogel such as native mucus.[21–24] By reason of the biochemical complexity, several functionalization as well as a good binding of both anionic and cationic cargos are achievable.[25]

In order to preserve the native functional properties of mucin, a time-consuming purification is usually required. Although it is known that the commercially available mucins lose some of their essential properties, such as its lubricity, due to the industrial purification processes, several studies describe covalently cross-linked hydrogels prepared from bovine submaxillary gland mucins (BSMs). Yan et al. have demonstrated a "clickable" mucin material by functionalizing BSM with tetrazine or norbornene via an inverse electron demand Diels–Alder cycloaddition reaction, revealing the value of mucin molecules in the field of immunomodulatory materials.[26,27] Two other reports describe covalently cross-linked hydrogels after the photochemical reaction of methacrylic-anhydride-modified mucin.[28,29] Both groups could synthesize hydrogels in this way with an elastic modulus similar to soft mammalian tissue.

For applications of the pig gastric mucin (PGM), usually a native form is used. This requires however a long purifying procedure where fresh pig stomachs are scraped out in a time-consuming manner followed by several purification steps, such as size exclusion chromatography or diafiltration.[30] There is also the possibility of the commercially available PGM which is used as gut model or to mimic adhesion in the digestion process.[31–34] A potential advantage of using commercially available PGM instead of BSM is its price, which is about 130 times lower than the latter one. The difference in comparison to BSM is that PGM has longer glycan chains but less terminal sialic acid than BSM.[12,35] This fact could cause the mucin-bound glycan to be different in some of the functionalities of the mucin hydrogels when PGM is used compared to other mucins.

Another natural macromolecule often used for hydrogel preparation is hyaluronic acid (HA). HA occurs naturally as an essential component of the ECM, which can be biodegraded in mammals by hyaluronidase.[36,37] Due to its functional groups, HA is modifiable and has been used, for example, by Dhanasingh et al. as a cross-linker in hydrogels after thiol functionalization in Michael addition systems.[38] Additionally, it was proven that HA can be used as an adjunct in inks for 3D printing due to its properties as a thickener.[39] In general, HA itself or the addition of HA is known to improve the biocompatibility or the cell behavior in different systems.[36]

In this work, we functionalized commercially available PGM with photoreactive groups, either with methacrylic anhydride or with allyl glycidyl ether. Subsequently, hydrogels prepared by two different cross-linking mechanisms were investigated and compared with respect to swelling behavior, mechanical properties, and cell compatibility. In this way, the disadvantages of commercially available PGMs such as gel forming properties, which recommend scraping fresh mucin from pig stomachs,[23,30] are not relevant to our study.

2. Results and Discussion

For the preparation of covalently cross-linked hydrogels, two different modifications of mucin with photoactive groups were undertaken. In the first one, PGM was methacrylated with methacrylic anhydride (MA), similar to previously published protocols for BSM.[28,29] In the second synthetic route, mucin was reacted with allyl glycidyl ether (AGE) via the alkaline-induced epoxy ring opening reaction in the aqueous solution. Both reaction schemes are presented in a simplified way in **Figure 1**.

The functionalization of PGM was in both cases reproducible, and the success of the reactions was assessed through ^{1}H-NMR (Figure S1, Supporting Information). Typical signals for the allyl function of the AGE-modified mucin and the methacryloyl group of the MA-modified mucins are at 6.0 ppm for –CH=CH_2 (e_2) and at 5.2 ppm corresponding to –CH=CH_2 (f_2).[40] Both MA as well as AGE can react with amine groups within the protein backbone or with hydroxyl groups present on the sugar chains. Unfortunately, neither Fourier transform infrared spectroscopy (Figure S2, Supporting Information) nor NMR provided a proof which reaction site was preferred. We assume however, that the bottlebrush-like structure of the mucin leads to the steric hindrance of the amine groups present in the protein backbone and a greater exposure of the hydroxyl groups present in the sugar chains. This results most likely that hydroxyl group in the glycans is preferably seen as reaction partner.

Subsequently, the two differently modified PGMs (Figure 1) were used for synthesizing hydrogels by covalent cross-linking in the photopolymerization process. Whereas PGM–MA homopolymer hydrogels were prepared via chain-growth free radical polymerization of the methacrylic groups, the radical step-growth thiol-ene click reaction of PGM–AGE (Figure 1) required an additional thiol containing component. Here, we used a thiol-functionalized hyaluronic acid (HASH) as a second polymeric constituent. In this reaction, a thioether linkage results from the dimerization reaction of a single thiol with a single allyl bond between two polymer chains that have been linked. Both kind of synthetic routes for preparation of hydrogels require UV irradiation and a presence of initiator. For both reactions 2-hydroxy-1-[4 (hydroxyethoxy)-phenyl]-2-methyl-1-propanone (Irgacure 2959) was used as initiator because of its moderate water solubility and low cytotoxicity.[41] Since cytotoxic effects of

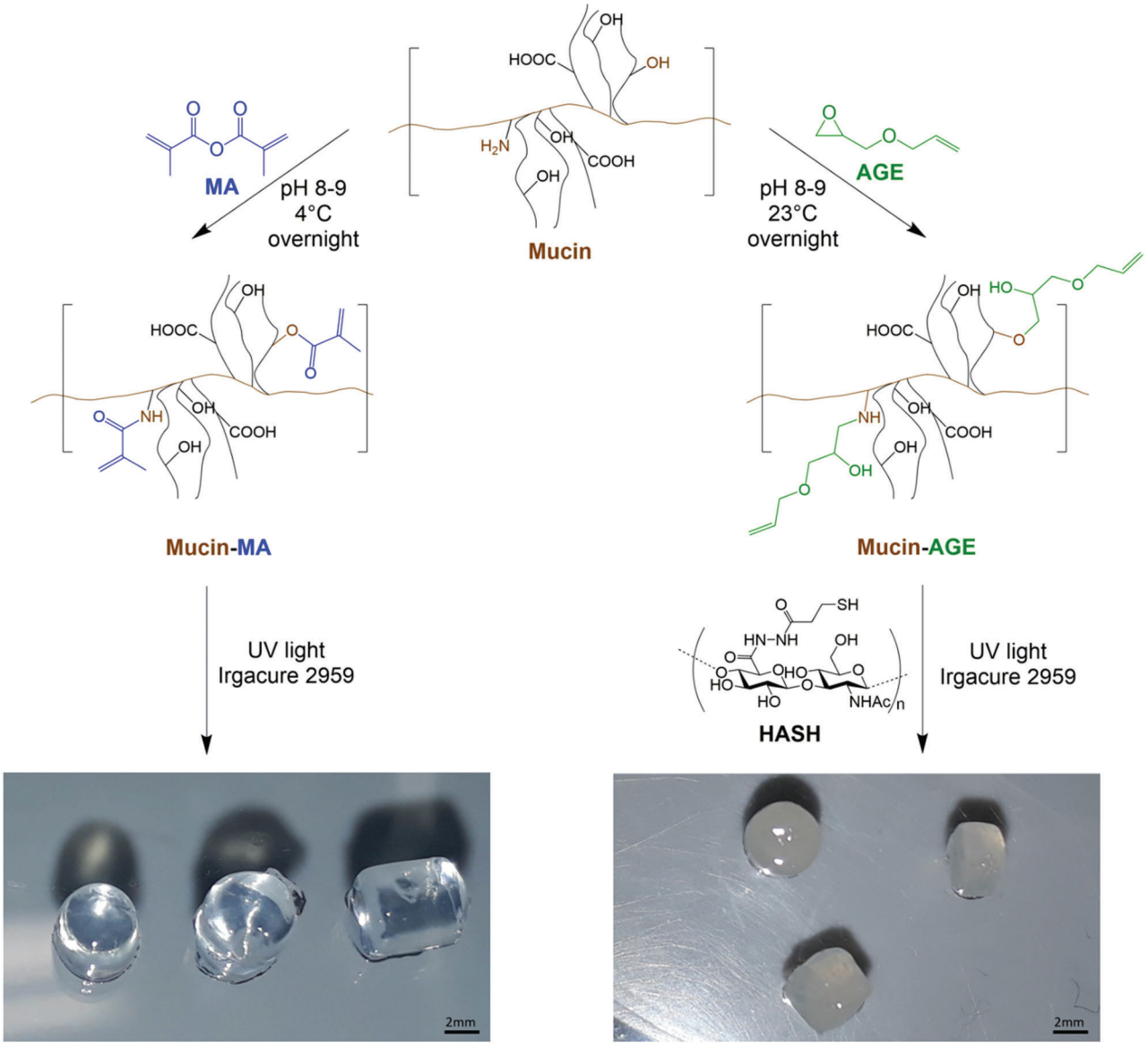

Figure 1. Modification of PGM and further processing to form-stable hydrogels. Simplified reaction scheme of the synthesis of PGM–MA and PGM–AGE. All theoretically possible reaction positions and reaction products after modification are shown. PGM–MA hydrogels (left, 4 × 4 mm molds), PGM–AGE–HASH hydrogels (right, 4 × 4 and 4 × 2 mm molds) with 0.5 mg mL^{-1} Irgacure 2959 after 1 min irradiation with UV light.

this photoinitiator over concentrations of 1 mg mL^{-1} were previously reported,[42–45] here, a concentration of 0.5 mg mL^{-1} was used. Together with Irgacure 2959 and UV light of the intensity of ≈6 mW cm^{-2}, hydrogels with a high shape fidelity could be obtained after irradiation (Figure 1). In this paper, we synthesized and studied three different hydrogels composed of 1) 4% w/v PGM–MA, 2) 4% w/v PGM–AGE–HASH (2% w/v PGM–AGE combined with 2% w/v HASH), and 3) 2% w/v PGM–AGE–HASH (1% w/v PGM–AGE combined with 1% w/v HASH). It is important to mention that no cross-linking was observed when PGM–AGE only (without thiol containing compound) was irradiated in the presence of initiator. In addition, hydrogels of methacrylated mucin with concentrations lower than 4% w/v could not be obtained.

For hydrogel characterization, swelling studies, mechanical testing, as well as determination of the pore size were performed. The swelling behavior of synthesized hydrogels was investigated in Milli-Q water as well as phosphate buffer saline (PBS) (**Figure 2**). It can clearly be seen that all types of hydrogels swell the most in the first hour and after almost 24 h the equilibrium, swelling is reached in both liquids. It is remarkable that the hydrogels nearly do not swell in PBS but that there is a significant difference to the strong swelling in Milli-Q water. This swelling behavior could be explained by the simple rules of osmosis. Milli-Q water is a hypotonic solution compared to the solution in the hydrogels and so the hydrogels gain water trough osmosis. Compared to this, the salt concentration in PBS provides an isotonic solution and has no or only a weak diffusion gradient into the

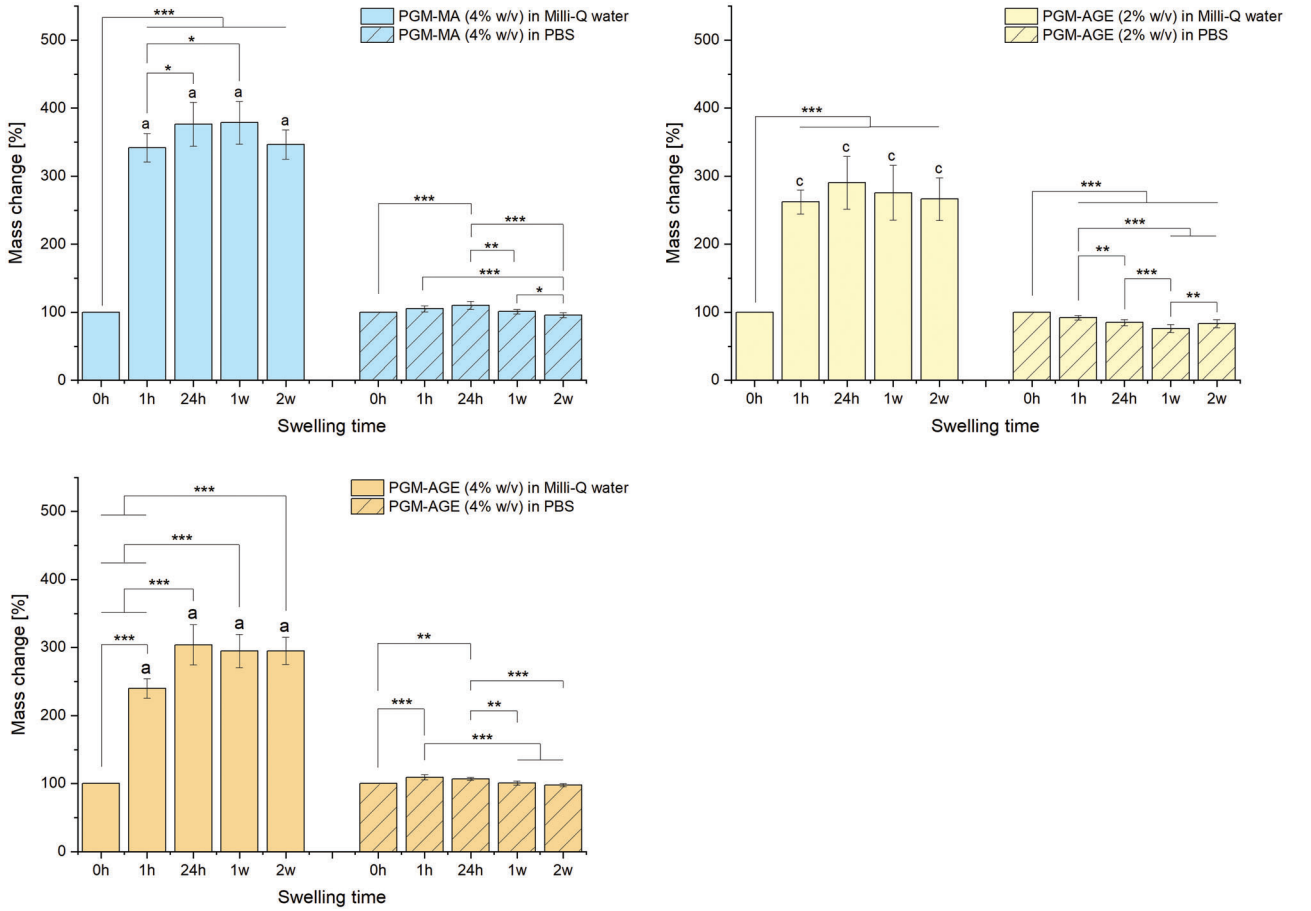

Figure 2. Swelling behavior of A) PGM–MA hydrogels and B,C) PGM–AGE–HASH hydrogels (B, 2% w/v and C, 4% w/v) in Milli-Q water (unpatterned) and in PBS (striped), (mean ± SD, $n = 6$). $^{a}p < 0.001$ versus the same sample swollen in PBS; $^{c}p < 0.05$ versus the same sample swollen in PBS; $^{***}p < 0.001$; $^{**}p < 0.01$; $^{*}p < 0.05$.

hydrogel. A volume change up to 60% more in water is literature known for other methacrylated hydrogels.[5]

Comparing the samples at 4% w/v (Figure 2, blue and orange), it is noticeable that the hydrogels prepared via chain-growth free radical polymerization swell to a higher extent in Milli-Q water than the thiol-ene cross-linked ones (100% → 300% compared to 100% → 400%). This is most likely due to the more heterogeneous network with defects resulting from not well-controllable cross-linking obtained by the polymerization of PGM–MA. As consequence, the methacrylated hydrogels are softer after some days, whereas the thiol-ene cross-linked hydrogels stay form-stable. In accordance with these results, swelling ratio of the hydrogels was determined by weighting the hydrogels before and after lyophilization after the same swelling times as mentioned at the swelling behavior (Figure S3, Supporting Information). The results of the swelling behavior could be confirmed by this study. Furthermore, by gravimetric analysis, it has been examined that 90–96% of the polymer is being converted during the reaction (exemplary shown for PGM–AGE–HASH hydrogels (2% w/v) in Table S1 in the Supporting Information).

For determination of the stiffness of the different hydrogels, the Young's modulus was determined by mechanical testing. The Young's modulus provides information about the density or the cross-linking degree of a hydrogel and it is known that a higher cross-linking results in stiffer hydrogels.[46,47] Therefore, in this work, the influence of the overall structure on the Young's modulus was investigated. All types of the here synthesized hydrogels were investigated after swelling in Milli-Q water (**Figure 3**) as well as in PBS. Based on the swelling results, the Young's modulus at time 0 h was expected to remain constant over the swelling time in PBS. This was nearly confirmed for all samples (Figure S4, Supporting Information).

It was assumed that the higher the concentration, the higher the cross-linking and the denser the network. Thus, less liquid can be absorbed by the hydrogel, and it shows a higher strength. This hypothesis was confirmed in the case of PGM–AGE where two different polymer concentrations were compared. It was also expected that thiol-ene reaction leads, because of its more controlled network formation, to stiffer hydrogels than free radical polymerization process.[46,47] Indeed, the less concentrated, 2% w/v, PGM–AGE–HASH hydrogels (Figure 3, yellow) have a similar stiffness as the 4% w/v PGM–MA (Figure 3, blue) materials. On the other hand, the PGM–AGE–HASH hydrogels with the same concentration as the PGM–MA hydrogels have a much higher stiffness (Figure 3, orange). Due to these results as well as the resulting swelling experiments, for later comparison

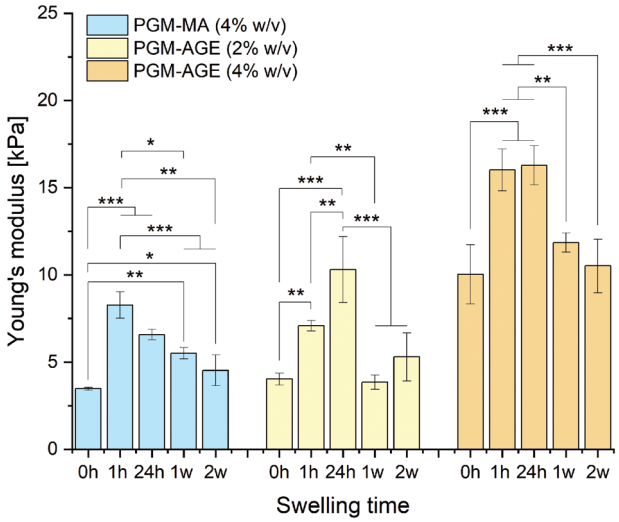

Figure 3. Young's moduli of PGM–MA hydrogels (blue), 2% w/v PGM–AGE–HASH hydrogels (yellow), and 4% w/v PGM–AGE–HASH hydrogels (orange) in Milli-Q water, (mean ± SD, $n = 6$). ***$p < 0.001$; **$p < 0.01$; *$p < 0.05$.

between free radical polymerization and thiol-ene reaction, always the 2% w/v PGM–AGE–HASH hydrogels were used.

The measured Young's moduli for all PGM hydrogels of around 3–18 kPa is in the range of native soft tissue and organs (0.1 kPa to 1 MPa), which enables later applications of these materials, such as on the skin for wound healing treatment or similar fields.[48]

In order to obtain more information about the pore size of the mucin hydrogels, diffusion experiments with fluorescently labeled dextran with molecular weights (Mws) between 40 and 250 kDa and larger were performed, similar to the earlier work of Duffy et al.[28] We observed that dextrans with Mw 250 kDa or larger are strongly retained by the PGM hydrogels (4% w/v PGM–MA and 2% w/v PGM–AGE–HASH) (Figure S5, Supporting Information). These observations suggest that the hydrogel pore size intermediate cutoff to is in the range between 4.78 and 11.46 nm.[28,49]

Cell experiments were performed with 4% w/v PGM–MA and 2% w/v PGM–AGE–HASH as these materials possess similar Young's moduli and swelling behavior. For detection of the metabolic activity of the respiratory chain of cultured cells after addition of the hydrogel's eluates, the water-soluble tetrazolium (WST) proliferation assay was used. Optical density and cell number were investigated with values over 80% and therefore proved as noncytotoxic (Figures S6 and S7, Supporting Information) In **Figure 4**, the total cell activity is shown for the eluates of the free radical polymerized hydrogels (left, striped) as well as for the thiol-ene cross-linked hydrogels (right, dotted). The cell activity is an indicator for how viable the remaining cells are in the eluates of the different hydrogels. Clearly, all samples show values over 80% (red line), indicating that the eluates of the mucin hydrogels are, referred to internal quality standards of this working group, not cytotoxic.

Cryo scanning electron microscopy (cryo-SEM) images were taken with the embedded cells within the hydrogels. A representative image is shown in Figure S8 (Supporting Information). It is known that structural changes may occur during the freezing process, therefore these images were taken only for illustration.

To further evaluate the cell compatibility in all of three hydrogels, L929 CCL1 murine fibroblasts as well as human mesenchymal stem cells (hMSCs) were encapsulated and cultured in vitro for several days. A live/dead staining was performed after 24 h, 7 days, 14 days, and 21 days in culture. After some days, the L929 cells begin to migrate to the rim of the hydrogel (Figure S9, Supporting Information). Whether for the methacrylated hydrogels or the thiol-ene cross-linked hydrogels, in both types of hydrogels, the cells slowly move to the edge and form agglomerates upon leaving the hydrogel after 21 days. For the methacrylated samples, it was observed that they were still form-stable after 21 days in cell medium but became very soft because of their swelling (Figure S10, Supporting Information). This made handling difficult, which is why only the two thiol-ene cross-linked hydrogels were investigated in cell experiments with hMSCs.

Generally, in **Figure 5** (exemplarily shown for the 4% w/v PGM–AGE–HASH hydrogels), it can be observed that cell elongation occurs, which is beneficial, as the spreading of cells in this 3D construct is necessary for cell differentiation. After 24 h, 70% viable cells could be detected. This number increased to 92% after incubation for 7 days. This may be due to the fact that the cells may have recovered from the demanding process of encapsulation after 7 days. Quantification after 14 days was beyond the scope of this study due to the nature of the sample and the elongated cells. However, it can be seen on the fluorescence images that more live cells are elongated than dead cells are noticeable.

The observed elongation of the cells is encouraging but rather unusual for mucin systems. For example, Yan et al. did not observe spreading or proliferation of their cells on mucin hydrogels.[27] The elongation observed here after 14 days may be due to the additional HA.

The WST content per µg DNA was also ascertained, as well as the DNA content per ng hydrogel (Figure S11, Supporting Information). Hereby, it could be confirmed that over the course of the cultivation, time less DNA is detectable in the hydrogel. Especially the behavior, that cells stay for a while in the protected surrounding hydrogel and then move out of the hydrogel, could be used for hydrogels as cell transport materials in tissue engineering approaches. The cells can be immobilized in the hydrogel in a protected manner, which improves the retention time in the target area in vivo. Depending on the type of injury, the implantation of cell-loaded hydrogels may be a suitable treatment method. This provides an optimized environment for infiltration, colonization, attachment, and proliferation, which could promote the synthesis of new extracellular matrix. The properties required for such an application are provided by the hydrogels.[50,51] Burdick et al. mentioned some examples of hydrogels as transport materials, in their study especially for stem cells. Until today, there is the challenge to recruit or position cells where desired and to control their survival and function in the postoperative treatment.[52]

3. Conclusions

In summary, this study demonstrates that it is possible to form cytocompatible hydrogels with tunable mechanical and swelling

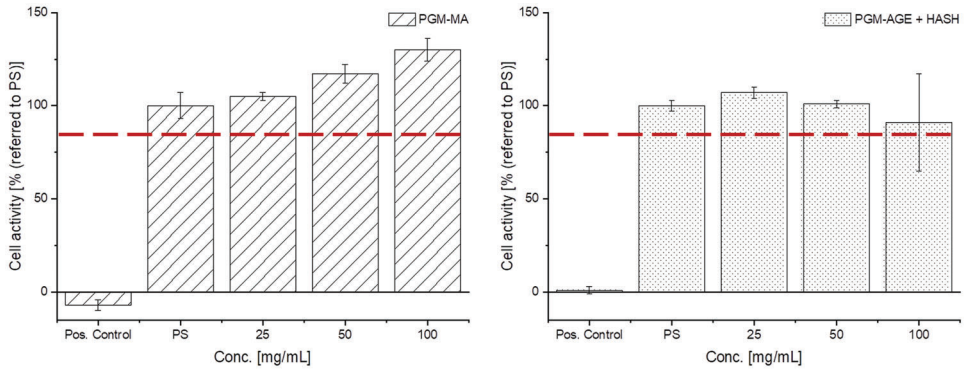

Figure 4. Cell activity (optical density/cell number) in % referred to the polystyrene positive control (100%). Differently concentrated eluate solutions (shown on the *x*-axis) were used to identify the point at which cytotoxic effects occur. Left, striped: PGM–MA (4% w/v) hydrogel eluates and right: 2% w/v PGM–AGE–HASH hydrogel eluates. The red line shows the 80% mark from which the samples are considered noncytotoxic according to internal quality standards.

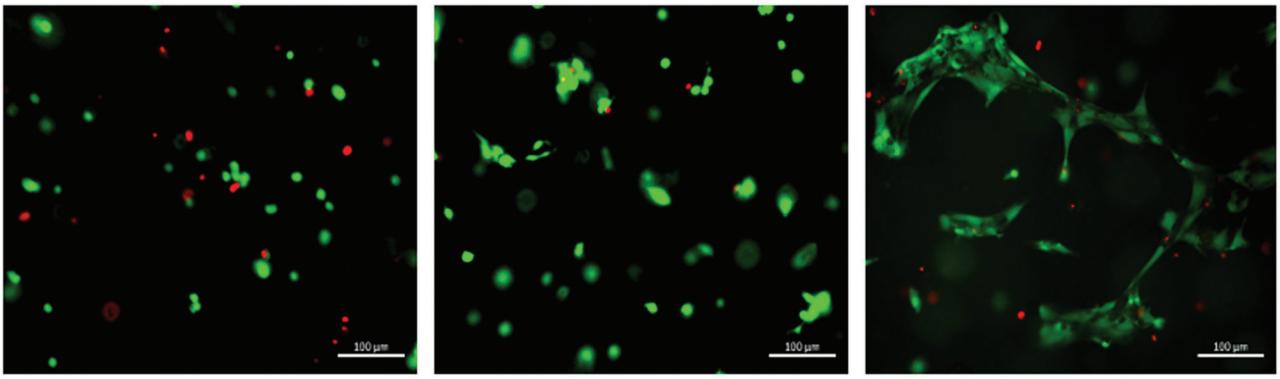

Figure 5. Cell viability of hMSCs, 24 h, 7 days, and 14 days after cross-linking, in 4% w/v PGM–AGE–HASH hydrogels. Viability assay is performed with an Irgacure 2959 concentration of 0.5 mg mL^{-1} and an irradiation time of 5 s. Viable cells are labeled with calcein acetoxymethyl ester and are depicted in green, dead cells are labeled with ethidium homodimer I and are depicted in red. Scale bar = 100 µm.

properties starting from a PGM which is normally dismissed as a waste product. It is possible to modify commercially available PGM with acrylates and allyl ether groups as photoreactive moieties in a reproducible manner. These two modifications allow hydrogel formation by free radical chain-growth polymerization of methacrylated groups as well as by thiol-ene reaction of allyl-ether-functionalized PGM with thiolated HA. Cell tests with the murine fibroblast cell line L929 CCL1 and with human MSCs confirm that neither the eluates of the hydrogels nor the hydrogels themselves show cytotoxic effects. It could be proved that the PGM hydrogels are cytocompatible and that cells are protected from external influences for a certain time before they migrate to the hydrogel's surface. This study thus lays the foundation for the further evaluation of applications for PGM hydrogels.

4. Experimental Section

Materials: Partially purified PGM (M1778) was purchased from Sigma-Aldrich and further purified according to published studies for BSM by Duffy et al., with little modifications.[28] PGM was dissolved at 40 mg mL^{-1} in Milli-Q water and centrifuged for 5 min with 4700 rpm. The supernatant was decanted to remove insoluble aggregates. It was further purified by dialysis (12–14 kDa cutoff) against Milli-Q water for 3 days with 3 water changes per day to remove protein contaminants. After lyophilization, a white solid could be obtained and stored at −20 °C. To avoid batch-to-batch variations during the following experiments, a large batch was purified and stored at −20 °C. BSM, MA, AGE (≥99%), sodium hydroxide, dipotassium phosphate, hydrochloric acid, disodium phosphate, monopotassium phosphate, fluorescein-isothiocyanate-labeled dextran (20, 40, 250, 500, 2000 kDa), and Irgacure 2959 were also obtained by Sigma-Aldrich, and used without further purifications. The radical photo initiator Irgacure 2959 was always used as fresh stock solution in water (3 mg mL^{-1}). PBS was custom made. For this, sodium chloride (8.00 g, 136 mmol), potassium dihydrogen phosphate (0.20 g, 1.47 mmol), sodium phosphate dibasic dodecahydrate (2.80 g, 7.82 mmol), and potassium chloride (0.20 g, 2.68 mmol) were dissolved in 1 L deionized water (all salts from Merck, Darmstadt, Germany). The pH was adjusted with 5 M NaOH or 5 M HCl solutions. HA (1–2 MDa), *N*-hydroxysuccinimide, ethyl (dimethylaminopropyl) carbodiimide hydrochloride, and dithiothreitol were purchased by CarboSynth. 3,3′-dithiobis(propanoic dihydrazide) was synthesized according to protocols of this working group. Dialysis tubes (molecular weight cut-off (MWCO) 1 and 12–14 kDa) were obtained by Spectrum Labs. Prior to use, dialysis tubes were always prewetted in Milli-Q water for at least 30 min. L929 CCL 1 murine fibroblasts (ATCC) were obtained via I. A. Z. Dr. Toni Lindl, Munich, Germany.

Mucin Modification—Mucin Methacrylation: The mucin methacrylation was conducted with PGM and MA. The procedure was varied from Duffy et al. as follows.[28] PGM was dissolved at 10 mg mL^{-1} in Milli-Q water. The solution was adjusted to a pH between 8 and 9 with 5 M sodium

hydroxide solution and cooled in an ice bath. MA was added at a final MA to mucin mass ratio of 1:1. The pH was controlled to stay stable, and the solution was stirred overnight at 4 °C. Subsequently, the solution was centrifuged for 3 min at 4700 rpm to remove excess MA and mucin precipitates and the supernatant was then dialyzed (12–14 kDa cutoff) against Milli-Q water for 3 days with 3 water changes per day. After lyophilization, the resulting mucin–MA was stored at −20 °C until further use.

Mucin Modification—Mucin Allylation: Modification of PGM with AGE was performed based on modified previous published protocols for gelatin[53] and the alkaline-induced epoxide ring opening. Mucin was dissolved at 40 mg mL^{-1} (1 eq) in Milli-Q water and the solution was adjusted with 5 M sodium hydroxide solution to a pH between 8 and 9. AGE was added in excess (1.1 eq). The solution was stirred overnight at 23 °C and afterward dialyzed (12–14 kDa cutoff) against Milli-Q water for 3 days with 3 water changes per day. After lyophilization, mucin–AGE was stored at −20 °C until further use.

The modified mucins were characterized based on ^{1}H-NMR spectroscopy with a 300 MHz Bruker Biospin spectrometer (Bruker, Billerica, MA, USA) and Fourier transform infrared spectroscopy with attenuated total reflection (ATR) (Thermo Scientific Nicolet iS10 with Smart iTR diamond ATR).

Hydrogel Formation—Via Free Radical Polymerization: Mucin–MA hydrogels were formed via the free radical polymerization process. For this, methacrylated mucin was dissolved at 40 mg mL^{-1} in Milli-Q water or PBS, respectively. For total dissolution, the mixture was stirred for 30 min at 23 °C. Then, Irgacure 2959 was added as photoinitiator as a stock solution in water (3 mg mL^{-1}) at a final concentration of 0.5 mg mL^{-1}. The solution was directly mixed by vortexing under light exclusion and then put into 4 × 4 mm custom made cylindrical silicone (poly(dimethysiloxane), PDMS) molds. The solution was then irradiated with UV light of 365 nm wavelength and a power of ≈6 mW cm^{-2} (bluepoint 4, Dr. Hoenle AG, Munich, Germany) for different times (5, 30, 60 s). The influence of exposure time was investigated for all samples before it was determined that the irradiation time of 60 s for 4 × 4 mm mold or 5 s for 1 × 6 mm mold was required. This light intensity was chosen because it is within the clinically acceptable range and is known to provide reasonable rates of polymerization.[54] After gelation, the hydrogels were taken out of the molds and placed in Milli-Q water or PBS, respectively, for later swelling studies, mechanical characterization, and cell viability studies.

Hydrogel Formation—Via Thiol-ene Reaction: Mucin–AGE hydrogels were formed, with HASH (385 kDa, degree of substitution (DS) 40%) (Scheme S1, Supporting Information) as thiol component, via the thiol-ene reaction. For this, the AGE-modified mucin as well as the HASH were dissolved in Milli-Q water or PBS, respectively, both to a final concentration of 10 mg mL^{-1}. Irgacure 2959 was added as photoinitiator as a stock solution in water (3 mg mL^{-1}) at a final concentration of 0.5 mg mL^{-1}. The further procedure was analogous to the hydrogel formation via free radical polymerization. The hydrogels were also used for later swelling studies, mechanical characterization, and cell viability studies.

Hydrogel Characterization—Mechanical Testing: To determine the stiffness of the different made hydrogels, triplicates of the hydrogels were fabricated each time 3 times ($n = 3^3$) as described above. Measurements were recorded after certain swelling times in linear compression using a BOSE 5500 system (ElectroForce, Eden Prairie, MN, USA) with a load cell of 250 g. The hydrogel cylinders (4 × 4 mm) were compressed parallel to their long axis with a constant crosshead displacement of 0.0005 mm s^{-1} till a total displacement of 1.5 mm. The Young's modulus was taken from the true stress–strain curve. For this, the slope was calculated from the raw data in the linear elastic range.

Hydrogel Characterization—Swelling Behavior: To obtain information about the network density, the swelling behavior, more exactly the swelling equilibrium and the maximum water uptake, was determined. For this, triplets of the different synthesized hydrogels were prepared as described above and incubated in PBS and/or Milli-Q water for specific times (0 h, 1 h, 24 h, 7 days, and 14 days). At the specific time points, the hydrogel was dried from each side, weighted, and put back into a fresh incubation solution. The 0 h value was set to 100% and the other values were calculated in regard to this.

Hydrogel Characterization—Swelling Ratio: The different synthesized hydrogels were also compared concerning their swelling ratio. The hydrogels were produced as mentioned before. For determination of the swelling ratio, the slightly modified protocol of Tibbitt et al. was used.[2] The hydrogels ($n = 6$) were lyophilized after 0 h, 1 h, 24 h, 7 days, and 14 days swelling in PBS or Milli-Q water at 23 °C. The hydrogels were directly weighted before and after lyophilization. The swelling ratio was calculated by dividing the swelling weight by the dried weight. When equilibrium swelling was reached, this value equaled Q (equilibrium swollen water weight over the dry weight).

Hydrogel Characterization—Gravimetric Analyses: Gravimetric analyses were performed to investigate the degree of polymer conversion during the cross-linking process. It was investigated whether the hydrogel loses weight during the swelling process by dissolving out nonreacted polymer. Hydrogel cylinders (4 × 4 mm) were prepared and weighed immediately after preparation. Afterward, the hydrogels were freeze-dried after various swelling times in water and weighted again. The maximum weight was determined by the composition of the hydrogels and the converted polymer was determined with the individual weights.

Cell Culture and Hydrogel Encapsulation—hMSCs: hMSCs are mesenchymal stem cells derived from human bone marrow. They were isolated from the cancellous bone of patients undergoing hip replacement surgery as approved by the local ethics committee of the University of Würzburg with the written consent of each donor patient. By thorough washing of the bone fragments and bone marrow with PBS, the hMSCs were released. This cell-containing suspension was centrifuged, the resulting cell pellet was resuspended in proliferation medium (Dulbecco's modified Eagle's medium (DMEM, GlutaMax, ThermoFisher Scientific)/F12, supplemented with 10% fetal calf serum (FCS, Sigma-Aldrich), 1% polystyrene, 50 µg mL^{-1} L-ascorbic acid-2-phosphate-sequimagnesium salt hydrate, and 5 ng mL^{-1} basic fibroblast growth factor (bFGF, BioLegend, London, UK)) and seeded into T175 cm^2 cell culture flasks (Greiner Bio-One, Frickenhausen, Germany). Careful washing with PBS removed the nonadherent cells after a few days. The adherent cells were cultivated at 37 °C and 5% CO_2 in proliferation medium up to subconfluent levels. Finally, the hMSCs were detached with 0.25% trypsin–Ethylenediaminetetraacetic acid (EDTA) and reseeded at a density of 3000–4000 cells cm^{-2}.

Cell Culture and Hydrogel Encapsulation—WST-1 Test: For the determination of cytotoxicity, a metabolic cell activity test with the cell proliferation agent WST-1 (Roche Diagnostics, Mannheim, Germany) was performed. For this, eluates of the differently produced hydrogels were prepared by covering the hydrogels with elution medium (1 mL medium per 0.1 g hydrogel) and incubating them for 48 h at 37 °C and 5% CO_2. For the elution medium, 1% 4-(2-hydroxyethyl)-1-piperazineethanesulfonic acid (HEPES, 1 M, ThermoFisher Scientific), 1% penicillin–streptomycin (ThermoFisher Scientific), and 10% FCS (Sigma-Aldrich) were added to DMEM (GlutaMax, ThermoFisher Scientific). As positive and negative controls, Vekoplan KT PVC plates (König GmbH, Wendelstein) and elution medium only were used, respectively. After incubation, the eluates were centrifuged, and the supernatant was additionally filtered through a 0.2 µm filter. The eluates were further diluted with elution medium to 50% and 25%. The culture medium of 48-well plates already containing adherent L929 CCL1 murine fibroblasts (ATCC, obtained via I. A. Z. Dr. Toni Lindl, Munich, Germany) was carefully aspirated and replaced by 500 µL of the corresponding eluate. The cells were then cultivated at 37 °C and 5% CO_2 for another 48 h. According to the manufacturer's instructions, the elution media were aspirated and a 1:10 dilution of the WST-1 reagent in cell culture medium (DMEM medium, Gibco) was added to each well. After incubation for 30 min at 37 °C and 5% CO_2, the supernatant was transferred into a new well plate. Since the adherent cells left behind were further used for cell number determination (see below), the monolayers were immediately covered with PBS. The extinction of the transferred WST-1 solution was measured with a Tecan Spark 20M plate reader (Tecan, Crailsheim, Germany) at 450 nm with a 690 nm reference filter. Samples exceeding the technical measuring range were diluted with PBS. For the determination of the cell numbers, L929 CCL1 murine fibroblasts were detached from the 48-well plates of the WST-1 assay. In detail, the cells were washed twice with PBS, covered with Accutase (Sigma-Aldrich), and incubated for

10 min at 37 °C. After resuspension in medium, the cell number mL^{-1} was determined with a Casy cell counter (OLS OMNI Life Science GmbH & Co KG).

Cell Culture and Hydrogel Encapsulation—WST-8 Assay and DNA Assay: For the determination of metabolic activity of hydrogel-encapsulated cells, a WST-8 assay (Cell Counting Kit 8, Sigma-Aldrich) was performed according to the manufacturer's manual. Briefly, hydrogels were washed twice in PBS and incubated in 250 µL of a WST-8 containing solution for 3 h at 37 °C and 5% CO_2. The metabolic activity was determined with a spectrophotometer (Tecan Spark 20M plate reader, Tecan, Crailsheim, Germany) at 450 nm and compared to a blank control. Following that, the hydrogels were washed twice in PBS and stored at −20 °C. For the analysis of DNA contents, the constructs were homogenized at 25 Hz for 5 min using a TissueLyser LT (Qiagen, Hilden, Germany) and afterward digested in 0.5 mL of a papain solution (3 U mL^{-1}) for 16 h at 60 °C. The DNA content of the hydrogels was determined by employing the Quant-iT PicoGreen double-stranded desoxyribonucleic acid (dsDNA) Reagent and Kit according to the manufacturer's manual. The DNA quantification was carried out fluorometrically at 485 and 538 nm using a Lambda DNA standard for quantification.

Cell Culture and Hydrogel Encapsulation—Viability Assay: The viability of encapsulated cells cultivated in their respective proliferation medium was examined on days 1, 7, 14, or 21. To detect viable cells, calcein acetoxymethyl ester (calcein-AM, Thermo Fisher) was used and dead cells were visualized with ethidium homodimer-I (EthD-I, Thermo Fisher). Therefore, the hydrogels with encapsulated cells were washed twice with PBS and incubated for 45 min at room temperature in the combined staining solution (1×10^{-6} M EthD-I, 2×10^{-6} M calcein-AM). The constructs were then washed with PBS and top view images were acquired with a fluorescence microscope (Axio Observer.Z1, equipped with epifluorescence optics and an MRm camera, Carl Zeiss, Jena, Germany).

Cell Culture and Hydrogel Encapsulation—Hydrogel Formation Including Cells: For cell experiments, all components for hydrogel formation had to be sterilized. This was done for PGM–MA, PGM–AGE, and HASH by irradiation with 254 nm for at least 30 min under sterile conditions. Sterile Milli-Q water and PBS were obtained by autoclaving. Irgacure 2959 stock solution was filtered through a sterile filter. The precursor solutions were then made analogous to the solutions without cells, like described before. Before placing them into the custom made 1 × 6 mm molds, cells (L929 cell line or hMSCs) were resuspended in the precursor solution. PGM–MA hydrogels as well as the 2% w/v PGM–AGE–HASH hydrogels were seeded with 5×10^5 L929 CCL1 murine fibroblasts mL^{-1}. For cross-linking of the hydrogels, the solution was then irradiated with UV light of 365 nm wavelength and a power of ≈6 mW cm^{-2} for different times (3, 5, 30 s). After gelation, the hydrogels including cells were taken out of the molds and placed into 12-well plates with proliferation media for a time period of 1, 7, and 21 days.

Cell Culture and Hydrogel Encapsulation—Cryo-SEM: For visualization of native hydrogel structures, cryogenic samples were prepared. For this purpose, pieces of the hydrogel were clamped between two aluminum plates ($d = 3$mm) with a notch of 2 mm diameter. By this, the hydrogel was enclosed and afterward quickly frozen in slushed nitrogen at −210 °C. The frozen samples were placed in a Leica EM VCT100 cryo-shuttle at −140 °C (Leica Microsystems ACE 400, Wetzlar, Germany) and transferred to the sputter coater. Here, the upper half of the sample was knocked off to get a fresh fractured surface and then freeze-etched at −85 °C for 15 min under vacuum ($<1 \times 10^{-3}$ mbar). The broken sample surface was then sputtered with 3 nm platinum and transferred with the cryo-shuttle into the chamber of a Crossbeam 340 field emission scanning electron microscope (Carl Zeiss Microscopy, Oberkochen, Germany). There, the morphology of the samples was imaged at −140 °C with an acceleration voltage of 8 kV.

Cell Culture and Hydrogel Encapsulation—Statistics: All data sets were first proved of normal distribution using the Kolmogorow test. Statistical analyses were carried out with SigmaPlot (Systat Software Inc.) using a one- or two-way analysis of variance followed by Tukey's post-hoc test. The data values were shown as mean values plus/minus standard deviation (SD). All results with a p-value below 0.05 were considered as significantly different.

Supporting Information

Supporting Information is available from the Wiley Online Library or from the author.

Acknowledgements

This work was supported by the German Research Foundation (DFG) within the collaborative research center TRR225 (project number 326998133 – subprojects B07, A02, and A06) and by the DFG State Major Instrumentation Program for funding the Zeiss Crossbeam CB 340 SEM (Grant No. INST 105022/58-1 FUGG).

Open Access funding enabled and organized by Projekt DEAL.

Conflict of Interest

The authors declare no conflict of interest.

Data Availability Statement

Research data are not shared.

Keywords

click chemistry, hydrogels, mucin, photopolymerization, thiol-ene

Received: July 10, 2021
Revised: October 19, 2021
Published online: January 27, 2022

[1] R. F. Pereira, P. J. Bártolo, *Engineering* **2015**, *1*, 090.
[2] M. W. Tibbitt, A. M. Kloxin, L. A. Sawicki, K. S. Anseth, *Macromolecules* **2013**, *46*, 2785.
[3] D. L. Elbert, A. B. Pratt, M. P. Lutolf, S. Halstenberg, J. A. Hubbell, *J. Controlled Release* **2001**, *76*, 11.
[4] C. E. Hoyle, C. N. Bowman, *Angew. Chem., Int. Ed. Engl.* **2010**, *49*, 1540.
[5] A. D. Rouillard, C. M. Berglund, J. Y. Lee, W. J. Polacheck, Y. Tsui, L. J. Bonassar, B. J. Kirby, *Tissue Eng., Part C* **2011**, *17*, 173.
[6] B. D. Fairbanks, M. P. Schwartz, A. E. Halevi, C. R. Nuttelman, C. N. Bowman, K. S. Anseth, *Adv. Mater.* **2009**, *21*, 5005.
[7] T. Billiet, E. Gevaert, T. De Schryver, M. Cornelissen, P. Dubruel, *Biomaterials* **2014**, *35*, 49.
[8] J. Zhu, R. E. Marchant, *Expert Rev. Med. Devices* **2011**, *8*, 607.
[9] S. Stichler, T. Jungst, M. Schamel, I. Zilkowski, M. Kuhlmann, T. Böck, T. Blunk, J. Teßmar, J. Groll, *Ann. Biomed. Eng.* **2017**, *45*, 273.
[10] G. Petrou, T. Crouzier, *Biomater. Sci.* **2018**, *6*, 2282.
[11] S. B. Destatis Fleischproduktion 2019 um 1,4% gegenüber dem Vorjahr gesunken, https://www.destatis.de/DE/Presse/Pressemitteilungen/2020/02/PD20_036_413.html#:~:text=WIESBADEN%20%2D%20Im%20Jahr%202019%20haben,8%2C0%20Millionen%20Tonnen%20Fleisch (accessed: april 2020).
[12] V. Bhavanandan, J. Hegarty, *J. Biol. Chem.* **1987**, *262*, 5913.
[13] R. Bansil, B. S. Turner, *Curr. Opin. Colloid Interface Sci.* **2006**, *11*, 164.
[14] B. Winkeljann, B. T. Käsdorf, J. Boekhoven, O. Lieleg, *Macromol. Biosci.* **2018**, *18*, 1700311.
[15] H. Ma, J. Hyun, P. Stiller, A. Chilkoti, *Adv. Mater.* **2004**, *16*, 338.
[16] T. Crouzier, H. Jang, J. Ahn, R. Stocker, K. Ribbeck, *Biomacromolecules* **2013**, *14*, 3010.

[17] A. S. Harti, S. D. Sulisetyawati, A. Murharyati, M. Oktariani, I. B. Wijayanti, *Int. J. Pharma Med. Biol. Sci.* **2016**, *5*, 76.
[18] L. Etim, C. Aleruchi, G. A. Obande, *Br. Microbiol. Res. J.* **2016**, *11*, 1.
[19] J. K. Nguyen, N. Masub, J. Jagdeo, *J. Cosmet. Dermatol.* **2020**, *19*, 1555.
[20] M. A. Momoh, S. A. Chime, D. U. Ogbodo, P. K. Akudike, S. U. Udochukwu, E. C. Ossa, F. C. Kenechukwu, K. C. Ofokans, A. A. Attama, *Trop. J. Pharm. Res.* **2021**, *18*, 927.
[21] O. Lieleg, I. Vladescu, K. Ribbeck, *Biophys. J.* **2010**, *98*, 1782.
[22] X. Cao, R. Bansil, K. R. Bhaskar, B. S. Turner, J. T. LaMont, N. Niu, N. H. Afdhal, *Biophys. J.* **1999**, *76*, 1250.
[23] J. P. Celli, B. S. Turner, N. H. Afdhal, R. H. Ewoldt, G. H. McKinley, R. Bansil, S. Erramilli, *Biomacromolecules* **2007**, *8*, 1580.
[24] L. D. Li, T. Crouzier, A. Sarkar, L. Dunphy, J. Han, K. Ribbeck, *Biophys. J.* **2013**, *105*, 1357.
[25] C. Kimna, T. M. Lutz, H. Yan, J. Song, T. Crouzier, O. Lieleg, *ACS Nano* **2021**, *15*, 2350.
[26] H. Yan, C. Seignez, M. Hjorth, B. Winkeljann, M. Blakeley, O. Lieleg, M. Phillipson, T. Crouzier, *Adv. Funct. Mater.* **2019**, *29*, 1902581.
[27] H. Yan, M. Hjorth, B. Winkeljann, I. Dobryden, O. Lieleg, T. Crouzier, *ACS Appl. Mater. Interfaces* **2020**, *12*, 19324.
[28] C. V. Duffy, L. David, T. Crouzier, *Acta Biomater.* **2015**, *20*, 51.
[29] A. Serafim, E. Olaret, S. Cecoltan, L. M. Butac, B. Balanuca, E. Vasile, M. Ghica, I. C. Stancu, *Mater. Plast.* **2018**, *55*, 68.
[30] V. J. Schömig, B. T. Käsdorf, C. Scholz, K. Bidmon, O. Lieleg, S. Berensmeier, *RSC Adv.* **2016**, *6*, 44932.
[31] J. Guerin, C. Soligot, J. Burgain, M. Huguet, G. Francius, S. El-Kirat-Chatel, F. Gomand, S. Lebeer, Y. L. Roux, F. Borges, *Colloids Surf., B* **2018**, *167*, 44.
[32] L. Li, E. Abou-Samra, Z. Ning, X. Zhang, J. Mayne, J. Wang, K. Cheng, K. Walker, A. Stintzi, D. Figeys, *Nat. Commun.* **2019**, *10*, http://doi.org/10.1038/s41467-019-12087-8
[33] N. Fernandez, L. Wrzosek, J. M. Radziwill-Bienkowska, B. Ringot-Destrez, M.-P. Duviau, M.-L. Noordine, V. Laroute, V. Robert, C. Cherbuy, M.-L. Daveran-Mingot, *Front. Physiol.* **2018**, *9*, 980.
[34] L. Li, Z. Ning, X. Zhang, J. Mayne, K. Cheng, A. Stintzi, D. Figeys, *Microbiome* **2020**, *8*, http://doi.org/10.1186/s40168-020-00806-z
[35] M. Scawen, A. Allen, *Biochem. J.* **1977**, *163*, 363.
[36] J. A. Burdick, G. D. Prestwich, *Adv. Mater.* **2011**, *23*, H41.
[37] M. N. Collins, C. Birkinshaw, *Carbohydr. Polym.* **2013**, *92*, 1262.
[38] A. Dhanasingh, J. Salber, M. Moeller, J. Groll, *Soft Matter* **2010**, *6*, 618.
[39] W. Schuurman, P. A. Levett, M. W. Pot, P. R. van Weeren, W. J. Dhert, D. W. Hutmacher, F. P. Melchels, T. J. Klein, J. Malda, *Macromol. Biosci.* **2013**, *13*, 551.
[40] T. Li, X. Tang, X. Yang, H. Guo, Y. Cui, J. Xu, *Asian J. Chem.* **2013**, *25*, 858.
[41] M. Liu, M. D. Li, J. Xue, D. L. Phillips, *J. Phys. Chem. A* **2014**, *118*, 8701.
[42] S. J. Bryant, C. R. Nuttelman, K. S. Anseth, *J. Biomater. Sci., Polym. Ed.* **2000**, *11*, 439.
[43] C. G. Williams, A. N. Malik, T. K. Kim, P. N. Manson, J. H. Elisseeff, *Biomaterials* **2005**, *26*, 1211.
[44] I. Mironi-Harpaz, D. Y. Wang, S. Venkatraman, D. Seliktar, *Acta Biomater.* **2012**, *8*, 1838.
[45] N. E. Fedorovich, M. H. Oudshoorn, D. van Geemen, W. E. Hennink, J. Alblas, W. J. Dhert, *Biomaterials* **2009**, *30*, 344.
[46] M. L. Oyen, *Int. Mater. Rev.* **2013**, *59*, 44.
[47] M. Galli, K. S. C. Comley, T. A. V. Shean, M. L. Oyen, *J. Mater. Res.* **2011**, *24*, 973.
[48] J. Liu, H. Zheng, P. S. Poh, H.-G. Machens, A. F. Schilling, *Int. J. Mol. Sci.* **2015**, *16*, 15997.
[49] J. K. Armstrong, R. B. Wenby, H. J. Meiselman, T. C. Fisher, *Biophys. J.* **2004**, *87*, 4259.
[50] F. P. W. Melchels, M. A. N. Domingos, T. J. Klein, J. Malda, P. J. Bartolo, D. W. Hutmacher, *Prog. Polym. Sci.* **2012**, *37*, 1079.
[51] P. J. Bártolo, C. K. Chua, H. A. Almeida, S. M. Chou, A. S. C. Lim, *Virtual Phys. Prototyping* **2009**, *4*, 203.
[52] J. A. Burdick, R. L. Mauck, S. Gerecht, *Cell Stem Cell* **2016**, *18*, 13.
[53] S. Bertlein, G. Brown, K. S. Lim, T. Jungst, T. Boeck, T. Blunk, J. Tessmar, G. J. Hooper, T. B. F. Woodfield, J. Groll, *Adv. Mater.* **2017**, *29*.
[54] S. Bryant, P. Martens, J. Elisseeff, M. Randolph, R. Langer, K. Anseth, in Chemical and Physical Networks: Formation and Control of Properties (Eds: B. T. Stokke, A. Elgsaeter), *The Wiley Polymer Networks Group Review Series*, Vol. 2, Wiley, New York **1999**, p. 395.